JOURNAL OF MATERIALS SCIENCE 35 (2000) 4293–4299

Sintering and crystallization of off-stoichiometric $SrO{\cdot}Al_2O_3{\cdot}2SiO_2$ glasses

YUN-MO SUNG*
Department of Materials Science and Engineering, Daejin University, Pocheon-koon, Kyunggi-do 487-711, South Korea
E-mail: ymsung@road.daejin.ac.kr

SUNGTAE KIM
Department of Materials Science and Engineering, University of Wisconsin-Madison, Madison, Wisconsin 53706, USA

Glass-ceramics with the celsian-corundum binary join composition of 88.8 wt% $SrO{\cdot}Al_2O_3{\cdot}2SiO_2$ – 11.2 wt% Al_2O_3, (SA2S-A), were fabricated by pressureless sintering and investigated for their sintering and crystallization behaviors. The (SA2S-A) glass powder showed crystallization peak and melting temperatures of ~1059 and 1550 °C, respectively and high sintering ability. The (SA2S-A) glass powders containing B_2O_3, (SA2S-A)B and those containing B_2O_3 and TiO_2, (SA2S-A)BT showed lowered crystallization peak temperatures of 1033 and 997 °C, respectively. By applying Kissiger analyses to the DTA data of the (SA2S-A), (SA2S-A)B and (SA2S-A)BT glass powders, the activation energy values for crystallization were determined as 488, 370 and 333 kJ/mol, respectively. The Ozawa analyses on the DTA data gave the Avrami parameter values at 1.2, 1.1 and 1.9, respectively for the (SA2S-A), (SA2S-A)B and (SA2S-A)BT glass powders. The x-ray diffraction (XRD) patterns of the (SA2S-A) glass-ceramics, crystallized at 1100 °C for 4 h, showed formation of both the monocelsian and hexacelsian phases. The (SA2S-A)B and (SA2S-A)BT glass-ceramics crystallized at 1100 °C for 1 h, showed formation of the phase-pure monocelsian and did not show any evidence of the hexacelsian formation prior to the monocelsian formation.

1. Introduction

The stoichiometric $SrO{\cdot}Al_2O_3{\cdot}2SiO_2$ (SA2S) composition forms two high-temperature crystalline forms of monocelsian and hexacelsian. The monocelsian has been studied mainly for the use as a matrix material for high-temperature ceramic composites [1, 2]. The major reasons of this include its high melting point of ~1650 °C, low thermal expansion coefficient of $\sim 2.5 \times 10^{-6}$/°C, oxidation resistance and phase stability up to the melting point [3–5]. On the other hand, the haxacelsian, a high-temperature metastable phase of the SA2S composition, shows high thermal expansion of $\sim 8 \times 10^{-6}$/°C and reversible phase transformations at ~600–800 °C which accompanied by volume expansion of ~3%. Therefore, the formation of the hexacelsian phase should be avoided in a high temperature structural application of the SA2S glass-ceramics.

Bansal *et al*. [3] fabricated stoichiometric (Sr, Ba)O·$Al_2O_3{\cdot}2SiO_2$ glass-ceramics by sintering and hot isostatic pressing (HIP). The SA2S glass-ceramic samples cold isostatic pressed and sintered, showed density values ranging from 66 to 98% of the theoretical value depending upon the final heating schedule. The SA2S glass-ceramic samples heated at 900 °C for 20 h showed formation of both the hexacelsian and monocelsian phases, while those heated at 1100 °C for 20 h showed only monocelsian phase. Bansal and Drummond [4] studied the kinetics of hexacelsian to monocelsian phase transformation using XRD technique and reported that the hexacelsian heated at 1100 °C for 30 h transformed to almost pure monocelsian. Hyatt and Bansal [5] also studied the crystallization kinetics of the stoichiometric SA2S glass powders and obtained the activation energy for hexacelsian crystal growth of 534 kJ/mol and Avrami parameter of 4.2. By using XRD technique they found that the phase transformation of hexacelsian to monocelsian occurs after 1 h heating at 1250 °C in the SA2S bulk glass. Thus, in order to obtain phase pure monocelsian SA2S glass-ceramics by sintering and crystallization the 1 h heating at 1250 °C or the 20 to 30 h heating at 1100 °C was needed. The heating temperature of 1250 °C is relatively too high and the heating time of 20 to 30 h is too long for application. Furthermore, to obtain a homogeneous SA2S glass melt a practical melting temperature of ~1800 °C is needed and this is a too high temperature for ceramic industries to obtain for the fabrication of wide range of glass-ceramics.

* Author to whom all correspondence should be addressed.

The lowered glass melting and crystallization temperatures can give huge benefit to the application of a glass-ceramic. Especially, for use as a substrate material in semiconductor packaging, a glass-ceramic which can be sintered and crystallized below the melting point of Au (1060 °C) or Cu (1080 °C), is highly required. By using these highly conductive metals in a pattern printing, one can solve the problems occurring in the use of high melting point and high resistance metals such as Mo or W. The lowered crystallization temperature also can supply easy fabrication for glass-ceramic matrix composites.

The crystallization temperature of a glass can be lowered by compositional changes. The addition of few weight percentage of nucleation agent such as TiO_2 or ZrO_2 can form finely distributed titanates or zirconates which can act as nuclei for the crystallization of a glass-ceramic phase [6–8]. A glass including the nuclei shows bulk crystallization behavior and a much lowered crystallization temperature. However, the addition of the nucleation agents can cause the premature crystallization of a glass before completion of sintering, resulting in low sintered density. Knickerbocker *et al*. [9] reported that the addition of a sintering aid such as B_2O_3 and P_2O_5 in a β-spodumene ($Li_2O{\cdot}Al_2O_3{\cdot}4SiO_2$) glass-ceramic can considerably reduce the glass viscosity above the glass transition temperature and improve the sintering ability of a glass. Sung [10] fabricated off-stoichiometric cordierite ($2MgO{\cdot}2Al_2O_3{\cdot}5SiO_2$) glass-ceramics containing both sintering aids (B_2O_3 and P_2O_5) and nucleation agent (TiO_2), and examined their composite effects. It was found that they have both high sintering ability and much lowered glass melting (∼1400 °C) and crystallization peak (∼900 °C) temperatures. The glass-ceramics also showed mechanical properties suitable enough for structural application [11].

The main focus of this study was the development of a phase-pure monocelsian glass-ceramic having lowered glass melting and crystallization peak temperatures, while maintaining high sintering ability. The glass-ceramics with the binary join composition of 88.8 wt% $SrO{\cdot}Al_2O_3{\cdot}2SiO_2$ − 11.2 wt% Al_2O_3, (SA2S-A), were produced by pressureless sintering and crystallization of glass powder pellets. Their sintering and crystallization behaviors were compared with those of the stoichiometric SA2S glass-ceramics studied by previous researchers. Also, the effect of sintering aid (B_2O_3) and nucleation agent (TiO_2) on the sintering and crystallization behaviors of the off-stoichiometric (SA2S-A) glass-ceramics was studied in detail.

2. Experimental procedure

High purity powders of $SrCO_3$, Al_2O_3, SiO_2, B_2O_3 and TiO_2 from Aldrich Chemical (Milwaukee, WI, USA) were used as starting materials. Table I lists the composition of each glass prepared for the present study. The (SA2S-A) composition corresponds to 88.8 wt% $SrO{\cdot}Al_2O_3{\cdot}2SiO_2$ − 11.2 wt% Al_2O_3. Fig. 1 shows an equilibrium phase diagram of the SrO-Al_2O_3-SiO_2 system [12]. For this system, the liquidus projection was not available and only the alkemade lines with binary and ternary compounds were presented on the phase diagram. The arrow on the diagram indicates the (SA2S-A) composition. The oxide powders were well mixed using a zirconia-ball milling. The powder mixture was loaded into a platinum crucible and placed in a resistance furnace with super Kanthal® heating elements for glass melting. The weight of target glass was 20 g. The powder mixture was calcined at 1000 °C for 1 h, further heated to 1600 °C for 1 h for complete glass melting, and quenched into distilled water. Clear glass fragments were obtained which were dried, hand ground using a high-purity alumina mortar and pestle, and zirconia-ball milled to the average particle size of 3–5 μm.

TABLE I Compositions of the stoichiometric SA2S and the off-stoichiometric glasses prepared for the present study

	Composition (wt%)				
Glasses	SrO	Al_2O_3	SiO_2	B_2O_3	TiO_2
(SA2S)	31.81	31.30	36.89	—	—
(SA2S-A)	28.24	39.01	32.75	—	—
(SA2S-A)B	27.40	37.83	31.77	3.00	—
(SA2S-A)BT	26.55	36.66	30.79	3.00	3.00

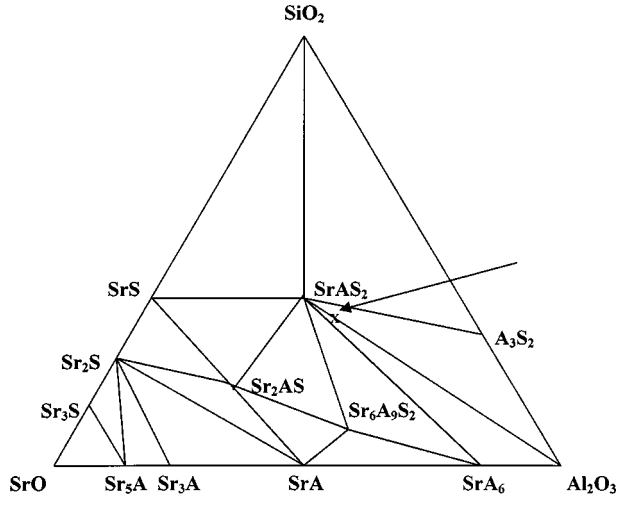

Figure 1 The equilibrium phase diagram of SrO-Al_2O_3-SiO_2 system showing only the alkemade triangles [12].

For each glass powder, various characteristic temperatures, such as glass transition (T_g), crystallization onset (T_o) and crystallization peak (T_p) were determined using differential thermal analyses (DTA: SETARAM TGDTA-92, France). The DTA results were analyzed for the activation energy and crystallization mode using the Kissinger [13] and Ozawa [14] analyses, respectively. These glass powders were cold pressed into pellets (4 mm-diameter and 2 mm-thickness) under pressure of 3000 psi, heated to 900 °C for 2 h for sintering, and heated to 1100 °C for 1, 2 and 4 h for crystallization. The sintering and crystallization heating was performed in air using the DTA at a heating rate of 20 °C/min.

The glass-ceramic pellets were analyzed for density using the Archimedes principle. Ten pellets out of each glass-ceramic composition were examined for the density and the averaged density values were obtained. The cross sections of the glass-ceramic pellets were polished using SiC papers (grit# 600 and 1000)

and alumina powders (1.0 and 0.3 μm). The polished samples were platinum coated by sputtering. The microstructure of the glass-ceramics was examined by scanning electron microscopy (SEM: JSM-6100, Jeol, Japan).

The x-ray diffraction (XRD: Nicolet Stoe Transmission/Bragg-Brentano, Stoe Co., Germany) was also performed on each of the powdered glass-ceramics crystallized at 1100 °C with a Cu-K_α source, a 5-s time constant, a 5–65° scan, and 0.05° step size. The phase identification was done by the comparison of the peak locations and intensities with the JCPDS cards (#38-1454 for monocelsian $SrO{\cdot}Al_2O_3{\cdot}2SiO_2$ and #35-73 for hexacelsian $SrO{\cdot}Al_2O_3{\cdot}2SiO_2$, and #10-173 for corundum Al_2O_3).

3. Results

By using XRD analyses apparent non-crystallinity was identified from the three glasses. DTA scan curves for the glasses at the heating rates of 10, 15, 20, 30 and 40°C/min are shown in Figs 2–4, respectively. In order to show the difference in the glass transition and crystallization DTA scan curves of the three glasses at a heating rate of 20 °C/min are compared in in Fig. 5. Table II lists the T_g, T_o and T_p values of the stoichiometric SA2S glass and the three non-stoichiometric (SA2S-A), (SA2S-A)B and (SA2S-A)BT glasses at a heating rate of 20 °C/min. The temperature values for the stoichiometric SA2S glass were taken from Hyatt and Bansal's data [5]. The off-stoichiometric (SA2S-A) glass showed T_g value 25 °C lower than that of the stoichiometric SA2S glass. The other off-stoichiometric glasses, (SA2S-A)B and (SA2S-A)BT, respectively

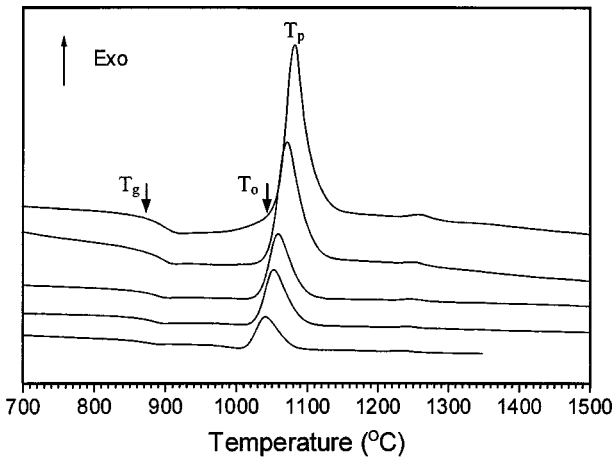

Figure 2 Differential thermal analysis (DTA) scan curves of the (SA2S-A) glass. The scan curves corresponds to the scan rates of 10, 15, 20, 30 and 40 °C/min, respectively from the bottom to the top.

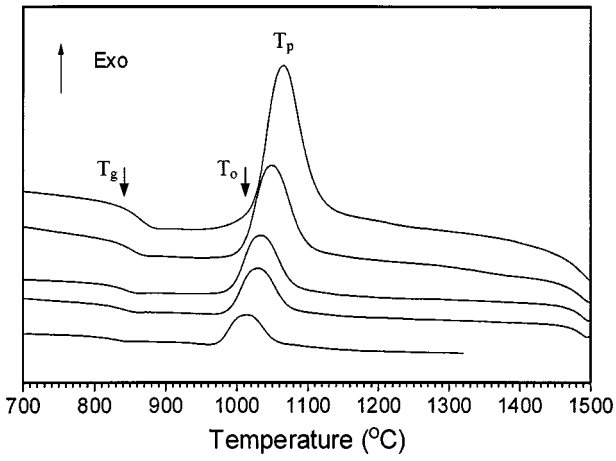

Figure 3 Differential thermal analysis (DTA) scan curves of the (SA2S-A)B glass. The scan curves corresponds to the scan rates of 10, 15, 20, 30 and 40 °C/min, respectively from the bottom to the top.

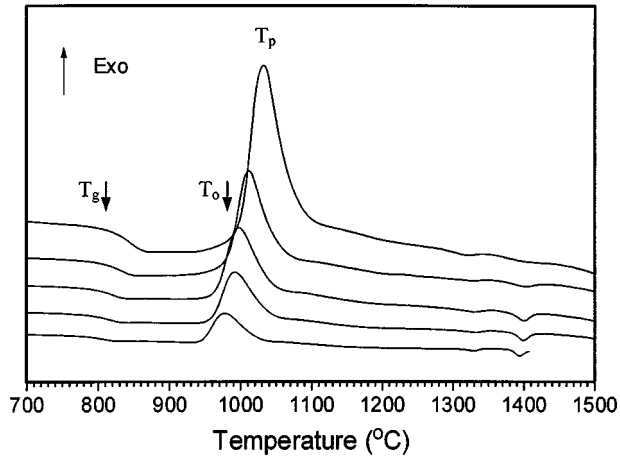

Figure 4 Differential thermal analysis (DTA) scan curves of the (SA2S-A)BT glass. The scan curves corresponds to the scan rates of 10, 15, 20, 30 and 40 °C/min, respectively from the bottom to the top.

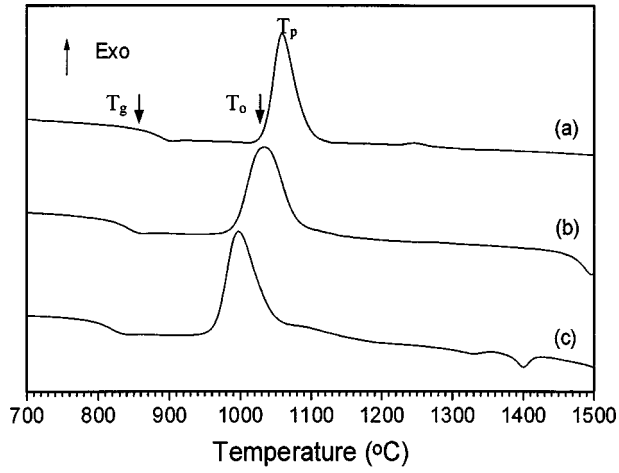

Figure 5 Comparison of the DTA scan curves of the (a) (SA2S-A), (b) (SA2S-A)B and (c) (SA2S-A)BT glasses at a scan rate of 20 °C/min.

TABLE II Summary of temperature values of the stoichiometric SA2S and the off-stoichiometric glass powders at a DTA scan rate of 20 °C/min

	Temperatures (°C)		
Glasses	Glass transition (T_g)	Crystallization onset (T_o)	Crystallization peak (T_p)
SA2S*	884	—	1053
(SA2S-A)	859	1036	1058
(SA2S-A)B	815	991	1033
(SA2S-A)BT	794	965	997

*The temperature values of the stoichiometric SA2S glass are from Hyatt and Bansal's DSC data [5].

showed T_g values which were 68 and 90 °C lower than that of the (SA2S-A) glass. The (SA2S-A) glass showed a T_p value 5 °C higher than that of the stoichiometric SA2S glass. The (SA2S-A)B and (SA2S-A)BT glasses, respectively showed T_p values 20 and 56 °C lower than that of the SA2S glass.

For the DTA scan curves the faster the heating rates, the higher the peak temperatures and the larger the peak heights become. The variation of T_p with the DTA scan rates can be used to estimate the activation energy for crystallization and crystallization mode. The activation energy values for crystallization of the glasses can be estimated by using following Kissinger analysis [13].

$$\ln\left(\frac{\phi}{T_p^2}\right) = -\frac{E_{ck}}{RT_p} + \text{const.} \qquad (1)$$

where ϕ is the DTA scan rate (°C/min), T_p is the crystallization peak temperature (°K), E_{ck} is the activation energy (kJ/mol) for the crystallization from Kissinger equation and R is the gas constant (8.3144 J/mol° K). From the Equation 1 the Kissinger plot of ln (ϕ/T_p^2) vs. $1000/T_p$ can be produced by substituting each DTA scan rate (ϕ) and its corresponding T_p value. Fig. 6 shows the Kissinger plots of (SA2S-A), (SA2S-A)B and (SA2S-A)BT glasses. The activation energy values for crystallization (E_{ck}) were determined from the slope ($-E_{ck}/R$) of each Kissinger plot. The activation energy values of (SA2S-A), (SA2S-A)B and (SA2S-A)BT glasses, were determined to be 488, 370 and 333 kJ/mol, respectively.

The crystallization mode of the glasses can be identified by using following Ozawa analysis [14].

$$\{\ln[-\ln(1-x)]\}_T = -n\ln\phi + \text{const.} \qquad (2)$$

where x is the volume fraction crystallized at a fixed temperature T when heated at ϕ that is, the ratio of the partial area at T to the total area of the crystallization exotherm. The n is the Avrami parameter which indicates a crystallization mode. The fixed temperature, T was 1070, 1050, and 1010 °C for the (SA2S-A), (SA2S-A)B and (SA2S-A)BT glasses, respectively. When surface crystallization dominates, $n\sim1$, and when bulk crystallization dominates, $n \geq 3$. When both the surface and bulk crystallization occurs n has a value between 1 and 3. By substituting ϕ values and corresponding x values into Equation 2 the Ozawa plots of the three glasses were created in Fig. 7. From the slopes of the Ozawa plots the Avrami parameter values of the (SA2S-A), (SA2S-A)B and (SA2S-A)BT glasses were determined as 1.2, 1.1 and 1.9, respectively. The DTA results were summarized in Table III.

The glass-ceramic pellets sintered at 900 °C for 2 h and crystallized at 1100 °C for 4 h, were analyzed for density using the Archimedes method. The averaged density values of the (SA2S-A) and (SA2S-A)B glass-ceramic pellets were 2.98 and 2.96, respectively while that of the (SA2S-A)BT glass-ceramic pellets was 2.78 g/cm^3.

The scanning electron micrographs (SEM) of the glass-ceramics are shown in Fig. 8. The microstructure of the (SA2S-A) and (SA2S-A)B glass-ceramics showed low porosity while that of the (SA2S-A)BT

TABLE III Summary of DTA results of the stoichiometric SA2S and the off-stoichiometric glass powders prepared for the present study

Glasses	Activation energy for crystallization, E_{ck} (kJ/mol)	Avrami parameter, n
SA2S*	534	4.2
(SA2S-A)	488	1.2
(SA2S-A)B	370	1.1
(SA2S-A)BT	333	1.9

*The activation energy for crystallization and Avrami parameter of the stoichiometric SA2S glass powder are from Hyatt and Bansal's result [5].

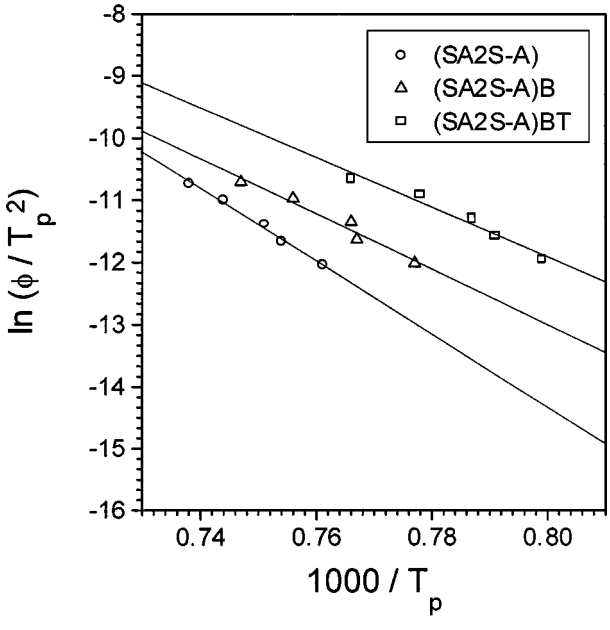

Figure 6 The Kissinger plots of the (SA2S-A), (SA2S-A)B and (SA2S-A)BT glasses. From the slopes of the lines the activation energy values for the crystallization were determined as 488, 370 and 333 kJ/mol, respectively.

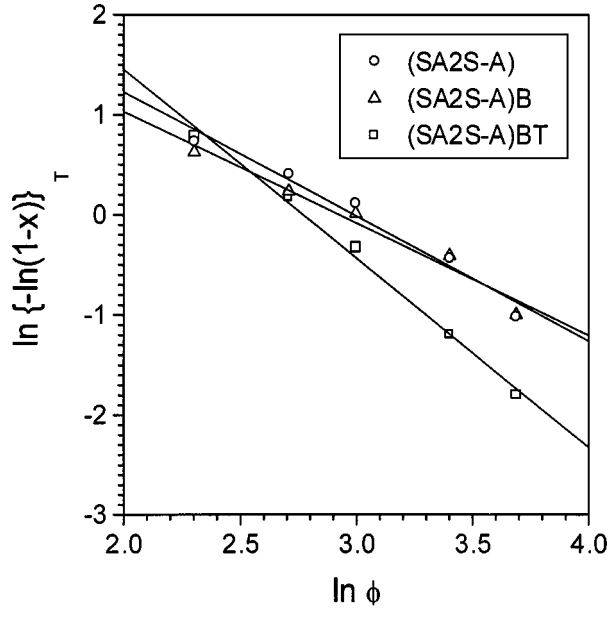

Figure 7 The Ozawa plots of the (SA2S-A), (SA2S-A)B and (SA2S-A)BT glasses. From the slopes of the lines the Avrami parameter values were determined to be 1.2, 1.1 and 1.9, respectively.

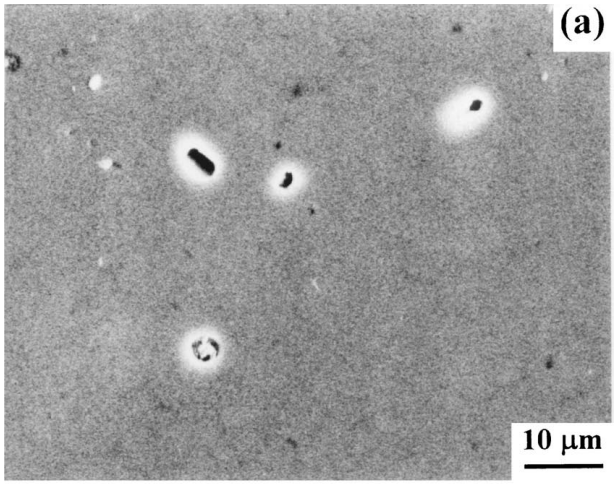

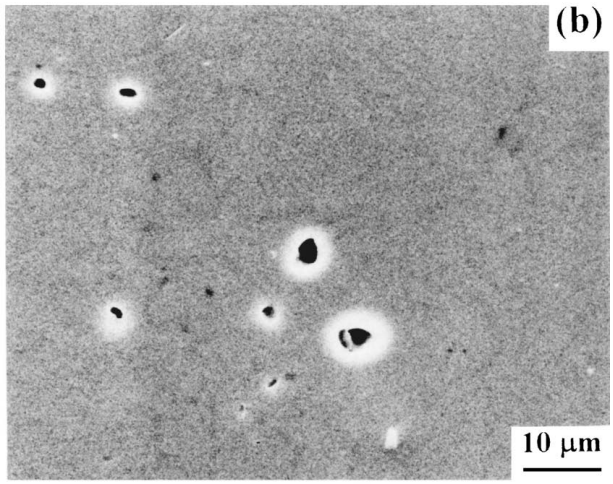

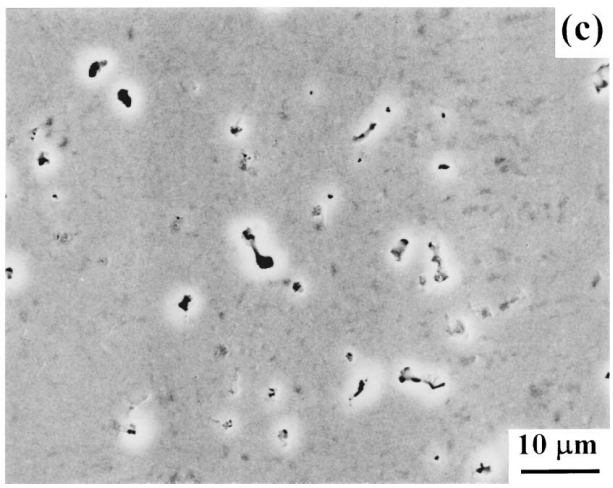

Figure 8 Scanning electron micrographs (SEM) of the (a) (SA2S-A), (b) (SA2S-A)B, and (c) (SA2S-A)BT glass-ceramics sintered at 900 °C for 2 h and crystallized at 1100 °C for 4 h.

glass-ceramics showed relatively high porosity which corresponds well with the density measurements.

In Fig. 9 the XRD patterns from the (SA2S-A) glass-ceramics sintered at 900 °C for 2 h and crystallized at 1000 °C for 4 h showed formation of both hexacelsian and monocelsian phases. On the other hand, (SA2S-A)B and (SA2S-A)BT glass-ceramics sintered at 900 °C for 2 h and crystallized at 1100 °C for 1 h, showed formation of only monocelsian phase. The formation of a crystalline Al_2O_3 phase was not identified.

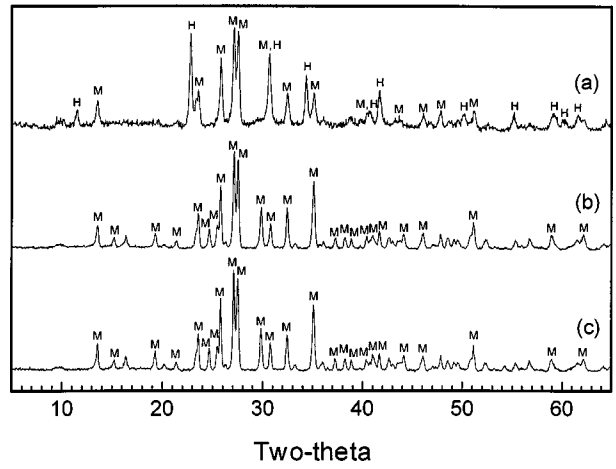

Figure 9 X-ray diffraction (XRD) patterns of the (a) (SA2S-A), (b) (SA2S-A)B and (c) (SA2S-A)BT glass-ceramics sintered at 900°C for 2 h and crystallized at 1000°C for 4 h. The (SA2S-A) glass-ceramic shows formation of both the hexacelsian (H) and monocelsian (M), while the (SA2S-A)B and (SA2S-A)BT glass-ceramics show only monocelsian (M).

4. Discussion

The practical melting temperature to obtain the homogenious (SA2S-A) glass melts was around 1600 °C which is much lower than the practical melting temperature (∼1800 °C) of the stoichiometric SA2S celsian composition. Due to this lowered melting temperature one can fabricate a glass-ceramic readily at less energy cost.

The glass transition and crystallization behaviors of a glass can give the key information to the glass-ceramic fabrication. According to the Hyatt and Bansal's DSC data[5] the glass transition temperature (T_g) of the stoichiometric SA2S celsian with a scan rate of 20 °C/min, was 884 °C while those of the glasses prepared for present study, (SA2S-A), (SA2S-A)B and (SA2S-A)BT were 859, 816 and 794 °C, respectively. The lowered glass transition temperature implies reduced viscosity of a glass. The effect of a sintering aid of B_2O_3 is apparent since the (SA2S-A)B and (SA2S-A)BT glasses, respectively show the T_g values lowered by 43 and 65 °C compared to the (SA2S-A) glass. The addition of B_2O_3 could reduce the strong connectivity of the three-dimensional chain structure of a silicate glass thus, can lower its glass viscosity.

The crystallization peak temperature (T_p) of the stoichiometric SA2S glass with a scan rate of 20 °C/min was 1053 °C while those of the (SA2S-A), (SA2S-A)B and (SA2S-A)BT glasses were 1059, 1033 and 997 °C, respectively. The crystallization of a glass can take place by the rearrangement of ions or molecules randomly oriented in it. Thus, a diffusion process is involved in the crystallization procedure. Since the (SA2S-A)B and (SA2S-A)BT glasses have low viscosity they can readily crystallize and thus, have lower crystallization peak temperatures (T_p's) compared to the (SA2S-A) glass. The addition of nucleation agent, TiO_2, seems to be very effective since the T_p of the (SA2S-A)BT glass was 36 °C lower than that of the (SA2S-A)B glasses. The TiO_2 must have formed titanates strongly acting as nucleation sites for the celsian phase.

The activation energy values for crystallization of $SrO{\cdot}Al_2O_3{\cdot}2SiO_2$ phase obtained by using the Kissinger method indicate that the glasses prepared for present study have lower values (488, 370 and 333 kJ/mol) than that (534 kJ/mol) [5] of the stoichiometric SA2S glass. This E_{ck} difference between the SA2S glass and the (SA2S-A) glass would be explained by the difference in the phase formation based on the XRD results. From the XRD patterns it was revealed that the (SA2S-A) glass forms both the hexacelsian and monocelsian phases at the 1100 °C heating while the stoichiometric SA2S glass only the hexacelsian. The fact that the (SA2S-A) glass has an activation energy value for crystallization lower than that of the SA2S glass implies that the activation energy for the monocelsian formation is lower than that for the hexacelsian formation. This statement can be strongly supported by the fact that the activation energy values for crystallization of the (SA2S-A)B and (SA2S-A)BT glasses forming only the monocelsian, are 370 and 333 kJ/mol, respectively which are much lower than that (534 kJ/mol) of the SA2S glass forming only the hexacelsian. The activation energy difference between the (SA2S-A)B and (SA2S-A)BT glasses would come from the existence of precursor nuclei most probably titanates such as $Al_2Ti_2O_7$ in a glass matrix. During the crystallization process the monocelsian phase can be formed with less amount of activation energy due to the nuclei preexisting in a glass matrix.

The crystallization mode of a glass has a practical importance in the usage of it and also in the fabrication of a glass-ceramic since the surface crystallization mode may introduce huge thermal expansion difference at the boundary between the glass phase and crystallized phase, building up high tensile stress [15]. This high tensile stress at the interface mostly causes total failure of the glass. On the other hand, in the case of the bulk crystallization mode where the crystal growth occurs at the finely distributed precursor nuclei in the glass, the huge thermal expansion coefficient gradient across the whole glass body does not occur, and the glass body is safe against the thermal failure. Thus, from this perspective the bulk crystallization is desirable compared to the surface crystallization. It is well known that in the production of glass-ceramics, nucleation agents such as TiO_2 and/or ZrO_2 are used to form titanates or zirconates finely distributed in a glass body. These precursor-nuclei finely distributed in a glass body can induce bulk crystallization and thus, a sound glass-ceramic body can be produced without a failure. The crystallization mode of a glass can be determined by the Avrami parameter value (n). The (SA2S-A) and (SA2S-A)B glasses showed approximately the same Avrami parameters of 1.2 and 1.1 which represent high surface crystallization tendency of them. Due to the existence of precursor nuclei the (SA2S-A)BT glass showed an Avrami parameter of 1.9 indicating the mixed crystallization mode.

The averaged density values of the (SA2S-A) and (SA2S-A)B glass-ceramics were 2.98 and 2.96 g/cm^3, respectively while that of the (SA2S-A)BT glass-ceramic was 2.78 g/cm^3. According to the XRD data both the (SA2S-A)B and (SA2S-A)BT glass-ceramics showed formation of only monocelsian and the (SA2S-A) glass-ceramic showed formation of monocelsian and hexacelsian. The glassy phase or corundum phase was not detected. Thus, the theoretical density of the glass-ceramics would be 3.084 g/cm^3. Each of the density values, thus, corresponds to 97, 96 and 90% of the theoretical density, respectively. The sintering ability of a glass can be estimated from the temperature range between crystallization onset and glass transition, $(T_o - T_g)$. The viscosity of a glass becomes to rapidly decrease when heated above the T_g at which the glass chain structure is broken. And then, it dramatically increases when crystallization initiates because the ions start to form highly ordered crystalline structure. Thus, the sintering of a glass occurs at the temperature range of $T_o - T_g$. If the temperature range is small a premature crystallization can occur before the completion of sintering. Once the premature crystallization occurs the viscosity of a glass increases tremendously and the sintering ends. Thus, high sintering ability can not be expected in a glass with a small temperature range of $T_o - T_g$. The $T_o - T_g$ values of the (SA2S-A), (SA2S-A)B and (SA2S-A)BT glasses at the DTA scan rate of 20 °C/min were 177, 176 and 171 °C, respectively. The (SA2S-A)BT glasses showed the smallest value since they would contain precursor nuclei such as titanates and during the sintering process a premature crystallization can occur. This result is in good agreement with density data.

The SEM micrographs of glass-ceramics well support the density measurements and DTA results. The (SA2S-A) and (SA2S-A)B glass-ceramics showed relatively low porosity compared to (SA2S-A)BT glass-ceramic. The addition of sintering aid, B_2O_3, seems not effective to the enhancement of the sintering ability of the (SA2S-A) glass. Most probably, lowered viscosity of a glass would have enhanced both sintering and crystallization of the glass. This statement can be strongly supported by the lowered T_g, T_p and E_{ck} values.

The XRD patterns of the (SA2S-A) glass-ceramics showed formation of the monocelsian and hexacelsian phases while those of the (SA2S-A)B and (SA2S-A)BT showed formation of only monocelsian phase. A broad hill indicating the existence of glassy phase was not detected which implies that the heating at 1100°C for 1–4 h was enough for the completion of crystallization of the glasses. The diffraction patterns from the corundum phase were not detected for all of the three glass-ceramics. Thus, it can be concluded that the glass-ceramics formed celsian solid solutions. The difference in the crystalline phase formation between the glass-ceramics would come from the viscosity difference between the glasses. Both the (SA2S-A)B and (SA2S-A)BT glasses contain B_2O_3 and their viscosity above the T_g would be reduced. The lowered viscosity would have enhanced formation of the monocelsian and depressed formation of the metastable hexacelsian phase. In order to confirm this, XRD was performed on the (SA2S-A)B and (SA2S-A)BT glasses heated to 1100 °C for only 1 s and quenched. The XRD patterns showed glass phase remained and the monocelsian phase formed as an only crystalline phase. This result reveals that the (SA2S-A)B and

(SA2S-A)BT glass-ceramics form the monocelsian phase directly from their glass matrices during the crystallization procedure. This result is contradictory to the result of Hyatt and Bansal [5] showing that in the stoichiometric SA2S glasses the formation of monocelsian phase occurs only through the phase transformation of hexacelsian. The depression of a metastable phase (μ-cordierite) formation by addition of B_2O_3 and TiO_2 was reported in the $2MgO \cdot 2Al_2O_3 \cdot 5SiO_2$ system as well [9]. This enhanced monocelsian formation with much shorter time period can supply high opportunity for the off-stoichiometric celsian glass-ceramics to be used for various applications.

5. Conclusions

The off-stoichiometric (SA2S-A) compositions were studied for the sintering and crystallization behaviors. The (SA2S-A) composition showed melting temperature $\sim$100 °C lowered compared to the stoichiometric SA2S composition. Due to the reduced viscosity the (SA2S-A)B and (SA2S-A)BT glasses, respectively, showed approximately 20 and 50 °C lowered crystallization peak temperature compared to the stoichiometric SA2S glass. The (SA2S-A)B and (SA2S-A)BT glasses formed the pure monocelsian phase at 1100 °C heating for only 1 h while the stoichiometric SA2S glass was known to form the monocelsian through the transformation of the hexacelsian at 1100 °C heating for 20–30 h. Due to the difference in the phase formation the (SA2S-A)B and (SA2S-A)BT glasses showed lower activation energy values for crystallization than the stoichiometric SA2S glasses. Avrami parameters of the (SA2S-A) and (SA2S-A)B glasses showed very close values of $\sim$1.0, which indicating strong surface crystallization tendency. The (SA2S-A)BT glass showed an Avrami parameter of 1.9 indicating mixed mode of surface and bulk crystallization. The (SA2S-A) and (SA2S-A)B glasses have bigger temperature range of $T_o - T_g$ than the (SA2S-A)BT glass and showed high sintering ability. In light of the lowered processing temperature, shorter processing time period, and high sintering ability the (SA2S-A)B glass-ceramics have high potential to be used for variety of applications.

Acknowledgements

This study was supported by 'San-Hak-Yon Consortium' of Daejin University in 1999.

References

1. N. P. BANSAL, *J. Mater. Res.* **12** (1997) 745.
2. *Idem., Mater. Sci. & Eng.* **A231** (1997) 117.
3. N. P. BANSAL, M. J. HYATT and C. H. DRUMMOND, III, *Ceram. Eng. Sci. Proc.* **12** (1991) 1222.
4. N. P. BANSAL and C. H. DRUMMOND, III, *J. Am. Ceram. Soc.* **76** (1993) 1321.
5. M. J. HYATT and N. P. BANSAL, *J. Mater. Sci.* **31** (1996) 172.
6. E. M. RABINOVICH, in "Advances in Ceramics, Vol. 4: Nucleation and Crystallization in Glasses," edited by J. H. Simmons, D. R. Uhlman and G. H. Beall (American Ceramic Society, Columbus, OH, 1982), p. 327.
7. V. MAIER and G. MULLER, *J. Am. Ceram. Soc.* **72** (1987) C-176.
8. Y.-M. SUNG, S. A. DUNN and J. A. KOUTSKY, *J. Eur. Ceram. Soc.* **14** (1994) 455.
9. S. KNICKERBOCKER, M. R. TUZZOLO and S. LAWHORNE, *J. Am. Ceram. Soc.* **72** (1989) 1873.
10. Y.-M. SUNG, *J. Mater. Sci.* **31** (1996) 5421.
11. *Idem., Ceram. Inter.* **23** (1997) 401.
12. P. S. DEAR, *Bull. Virginia Polytechnic Inst.* **50** (1957) 8.
13. H. E. KISSINGER, *J. Res. Natl. Bur. Stand.* (US) **57** (1956) 217.
14. T. OZAWA, *Polymer* **12** (1971) 150.
15. Y.-M. SUNG and J.-H. SUNG, *J. Mater. Sci.* **33** (1998) 4733.

Received 7 September 1999
and accepted 22 February 2000